



# Patterns and Drivers of *nirK*-Type and *nirS*-Type Denitrifier Community Assembly along an Elevation Gradient

Yongping Kou,<sup>a</sup> Yanjiao Liu,<sup>b</sup> Jiabao Li,<sup>a</sup> Chaonan Li,<sup>a</sup> Bo Tu,<sup>a</sup> Minjie Yao,<sup>b</sup> Xiangzhen Li<sup>a\*</sup>

<sup>a</sup>Key Laboratory of Environmental and Applied Microbiology, CAS, Environmental Microbiology Key Laboratory of Sichuan Province, Chengdu Institute of Biology, Chinese Academy of Sciences, Chengdu, China

<sup>b</sup>Engineering Research Center of Soil Remediation of Fujian Province University, College of Resources and Environment, Fujian Agriculture and Forestry University, Fuzhou, China

**ABSTRACT** *nirK*-type and *nirS*-type denitrifier communities mediate the conversion of nitrite to nitric oxide, which is the key step in denitrification. Results of previous studies have indicated that *nirK*-type and *nirS*-type denitrifiers may occupy different niches; however, the mechanisms and drivers of their responses to environmental changes within community assembly are poorly understood. In this study, we evaluated the distribution and assembly of *nirK*-type and *nirS*-type denitrifier communities along an elevation gradient from 1,800 to 4,100 m at Mount Gongga, China. Results showed that elevational patterns of alpha diversity in *nirK*-type and *nirS*-type denitrifier communities followed hump-backed patterns along the elevation gradient. However, *nirK*-type denitrifier communities formed two distinct clusters that were primarily separated by elevation, whereas *nirS*-type denitrifier communities formed three distinct clusters that were primarily separated by forest type along the elevation gradient. Moreover, deterministic processes were dominant in governing the assemblages of *nirK*-type and *nirS*-type denitrifiers. Soil pH was a key factor influencing the alpha and beta diversity of the *nirK*-type denitrifier communities, whereas plant richness was a primary variable influencing *nirS*-type denitrifiers. Additionally, our work revealed that soil denitrification potential was mainly explained by the variation in the beta diversity of denitrifier communities rather than the alpha diversity of denitrifier communities or denitrifier abundances over a large elevation gradient, and *nirK*-type denitrifiers played more important roles in soil denitrification. These results may contribute to predicting the consequences of global changes on denitrifier communities and their ecological services.

**IMPORTANCE** Mount Gongga is the highest peak in the Hengduan Mountain region and is located at the southeastern fringe of the Tibetan Plateau, Sichuan Province, southwest China. As a transitional zone between the Tibetan Plateau and Sichuan Basin, Gongga Mountain features particularly diverse topography, geology, climate, and biodiversity and is a globally significant hot spot of biodiversity. In this contribution, we comprehensively describe the diversity and assembly of denitrifier communities along an elevation gradient on Gongga Mountain. Our findings established for the first time that the distribution patterns of beta diversity and driving factors differed between *nirK*-type and *nirS*-type denitrifier communities, and deterministic processes were dominant in shaping communities of denitrifiers. Moreover, the beta diversity of denitrifier communities rather than alpha diversity or denitrifier abundance played an important role in explaining denitrification potential, and the beta diversity of *nirK*-type denitrifier communities was more important than *nirS*-type denitrifier communities in soil denitrification. This work provides crucial insights into the spatial distribution of denitrifier communities and their ecological function and increases our understanding of the mechanisms underlying spatial distribution of community assembly along large elevation gradients.

**Citation** Kou Y, Liu Y, Li J, Li C, Tu B, Yao M, Li X. 2021. Patterns and drivers of *nirK*-type and *nirS*-type denitrifier community assembly along an elevation gradient. *mSystems* 6:e00667-21. <https://doi.org/10.1128/mSystems.00667-21>.

**Editor** Theodore M. Flynn, California Department of Water Resources

**Copyright** © 2021 Kou et al. This is an open-access article distributed under the terms of the [Creative Commons Attribution 4.0 International license](https://creativecommons.org/licenses/by/4.0/).

Address correspondence to Xiangzhen Li, [lixz@biobit.net.cn](mailto:lixz@biobit.net.cn).

\*Present address: Xiangzhen Li, Chengdu Institute of Biology, Chinese Academy of Sciences, Chengdu, China.

**Received** 11 June 2021

**Accepted** 29 September 2021

**Published** 2 November 2021

**KEYWORDS** *nirK*-type denitrifiers, *nirS*-type denitrifiers, community assembly, elevation gradient, denitrification potential

Soil denitrifiers are crucial in the reduction of nitrate ( $\text{NO}_3^-$ ) and/or nitrite ( $\text{NO}_2^-$ ) to gaseous nitrogen ( $\text{N}_2$ ) during denitrification (1). The reduction of  $\text{NO}_2^-$  to nitric oxide (NO), the key step in denitrification, is catalyzed by nitrite reductase encoded by the *nirK* or *nirS* gene (2). Therefore, *nirK* and *nirS* are typically used as effective marker genes for characterizing the abundances and community composition of denitrifiers in ecosystems (3, 4). These two genes are considered mutually exclusive among denitrifiers (5), and most denitrifiers possess either *nirK* or *nirS*, although a few strains have been reported to possess both genes (6). In addition, these two genes are thought to occur in two ecologically distinct denitrifying groups, and denitrifiers with *nirK* and *nirS* genes may differ in different denitrification abilities (7–9). However, the linkages among biogeographic distributions, assembly processes, and key drivers of soil denitrifier communities as well as the potential denitrification rate (PDR) in ecosystems remain unclear.

Previous studies have shown that *nirK*-type and *nirS*-type denitrifier communities in estuary, watershed, and agricultural ecosystems respond differently to environmental variables, such as soil type, climate, organic carbon, nitrate, plants, oxygen concentration, and salinity (7, 10–12). For example, Azziz et al. (10) reported that *nirS*-type denitrifier communities are more sensitive than the *nirK*-type denitrifiers to soil type, rice cultivar, and water management. Moreover, *nirS*-type denitrifiers are more likely to be influenced by plant species than *nirK*-type denitrifiers in terrestrial ecosystems (11, 13–15). Plant communities influence soil microbial assemblages either through the effects of rhizodeposits or the alteration of soil conditions (11, 16). Indeed, Hou et al. (11) showed the *nirS*-type denitrifiers to be more sensitive than *nirK*-type denitrifiers to the rhizosphere effect in agricultural soils and proposed that root exudates, acting as inducible carbon sources, can exhibit different effects on *nirS*-type and *nirK*-type denitrifier communities. In contrast, a previous study reported a stronger effect on *nirK*-type denitrifiers than *nirS*-type denitrifiers in the rhizosphere of a wetland plant (17). Similarly, soil pH also shows different effects on the abundances and communities of *nirK*-type and *nirS*-type denitrifiers in various ecosystems (4, 18, 19). For example, *nirS*-type denitrifier communities are more sensitive to pH gradients (ranging from pH 4.2 to 6.6) than are *nirK*-type denitrifiers under a long-term (50 years) pH manipulation (4). In addition, Ligi et al. (20) reported that the abundance of the *nirS* gene, but not that of the *nirK* gene, was affected by soil pH in a constructed riverine wetland complex. These inconsistent results may be attributed to different selection mechanisms for various denitrifiers in specific ecosystems.

Community assembly processes include deterministic and stochastic processes (21, 22). According to the framework described in previous studies (21), deterministic processes include heterogeneous and homogenous selection, whereas stochastic processes include dispersal limitation, homogenizing dispersal, and drift. Homogeneous selection (under homogeneous conditions) results in lower variation in community structure or species/compositional turnover, whereas heterogeneous selection under heterogeneous environmental conditions produces high variation in community structure. Mountain ecosystems exhibit great changes in climate, plant parameters, and soil properties over short spatial distances, which can be used as analogs to environmental gradients to understand microbial activity, community assembly, and their relationships with environmental factors. Previous studies have revealed that deterministic processes (heterogeneous selection) dominate in the assembly processes of soil microbial communities (including communities of soil bacteria, diazotrophs, and methanotrophs) along a large altitudinal gradient, among which climate, plant, and soil parameters play important roles in shaping microbial communities (23–25). Moreover, along with environmental factors (such as temperature and plant parameters) that covary with elevation and could influence the distribution patterns of soil microbial communities (23, 26), geological processes (such as parent rock and weathering) explain additional variation in plant and microbial communities

(27). However, the relative contributions of deterministic versus stochastic processes in the assemblies of *nirK*-type and *nirS*-type denitrifier communities along large elevation gradients remain unknown.

Various elevational biodiversity (species richness) patterns of soil bacterial communities (23, 28–30) and functional microbial groups, e.g., diazotrophs (25) and methanotrophs (24), have been observed, suggesting that microbial diversity patterns along elevation gradients are ecosystem specific and scale dependent. However, previous studies have primarily focused on the changes in elevational biodiversity patterns in terms of species richness ( $\alpha$ -diversity), and the elevational changes in microbial community turnover ( $\beta$ -diversity) have been much less studied (31). Moreover, some studies have suggested that the  $\beta$ -diversity of denitrifier communities is a more robust indicator for interpreting the variation in PDR than denitrifier abundances in arid and semiarid regions (32, 33). However, denitrifier gene (*nirK* or *nirS*) abundances, but not denitrifier communities, are reported to be good predictors of PDR (1, 34). For example, studies have reported PDR to be correlated with the abundance of *nirS*-type denitrifiers or *nirK-nirS* gene abundance in fertilized grassland soil (35) and in soils from a permafrost black spruce forest to a rich fen (1), whereas another study also found PDR to be positively correlated with the abundance of *nirK*-type denitrifiers but not correlated with changes in corresponding community composition in forest soils (34). In addition, previous studies have suggested that *nirS*-type denitrifiers are more likely to be capable of complete denitrification under suitable conditions than are *nirK*-type denitrifiers (36). Therefore, *nirS*-type denitrifiers may play more important roles in denitrification, since they can produce greater quantities of denitrification enzyme than can the *nirK* community (4). However, the relative contributions of *nirK*-type and *nirS*-type denitrifier communities/abundances to PDR remain poorly understood along elevation gradients.

Mount Gongga is the highest mountain on the eastern boundary of the Tibetan Plateau. The drastic environmental changes along the elevation gradient on the eastern slope of Mount Gongga offer a unique platform for investigating the biogeographical distributions of *nirK*-type and *nirS*-type denitrifiers and the ecological processes regulating community assembly over such a large elevational scale. Hence, our primary objectives were to compare the biogeographical distributions, assembly processes, and key driving factors of the variations of *nirK*-type and *nirS*-type denitrifiers and to assess the relationships between variation in *nirK*-type and *nirS*-type denitrifiers and PDR along the elevation gradient. Specifically, we hypothesized (i) that deterministic processes (heterogeneous selection) dominate the assembly processes of denitrifier communities and that soil pH and plant parameters are the key environmental factors shaping *nirK*-type and *nirS*-type denitrifier communities along an elevation gradient, and (ii) that PDR is mainly explained by variation in the beta diversity of denitrifier communities rather than by denitrifier abundances or the alpha diversity of denitrifier communities along a large elevation gradient and that *nirS*-type denitrifiers play more important roles in soil denitrification.

## RESULTS

**Climate, plant, and soil properties along the elevation gradient.** The mean annual temperature (MAT) decreased and the mean annual precipitation (MAP) increased with elevated altitude. The average total carbon (TC), total nitrogen (TN), extractable nitrate ion ( $\text{NO}_3^-$ ), and conductivity were significantly higher at low elevations (1,800 to 2,800 m) than those at high elevations (3,000 to 4,100 m). Soil pH (ranging from 3.53 to 7.23) was significantly higher at 1,800 to 2,600 m than at 2,800 to 4,100 m. The extractable ammonium ion ( $\text{NH}_4^+$ ) levels varied from 1.81 to 62.78 mg (kg dry weight soil)<sup>-1</sup> along the elevation gradient. Among the woody plant species, the evergreen broadleaf trees (EB), the deciduous broadleaf trees (DB), and dark coniferous trees (DC) exhibited an uneven distribution at all elevations. Plant richness first decreased and then increased with increasing altitude. These data were from Li et al. (23).

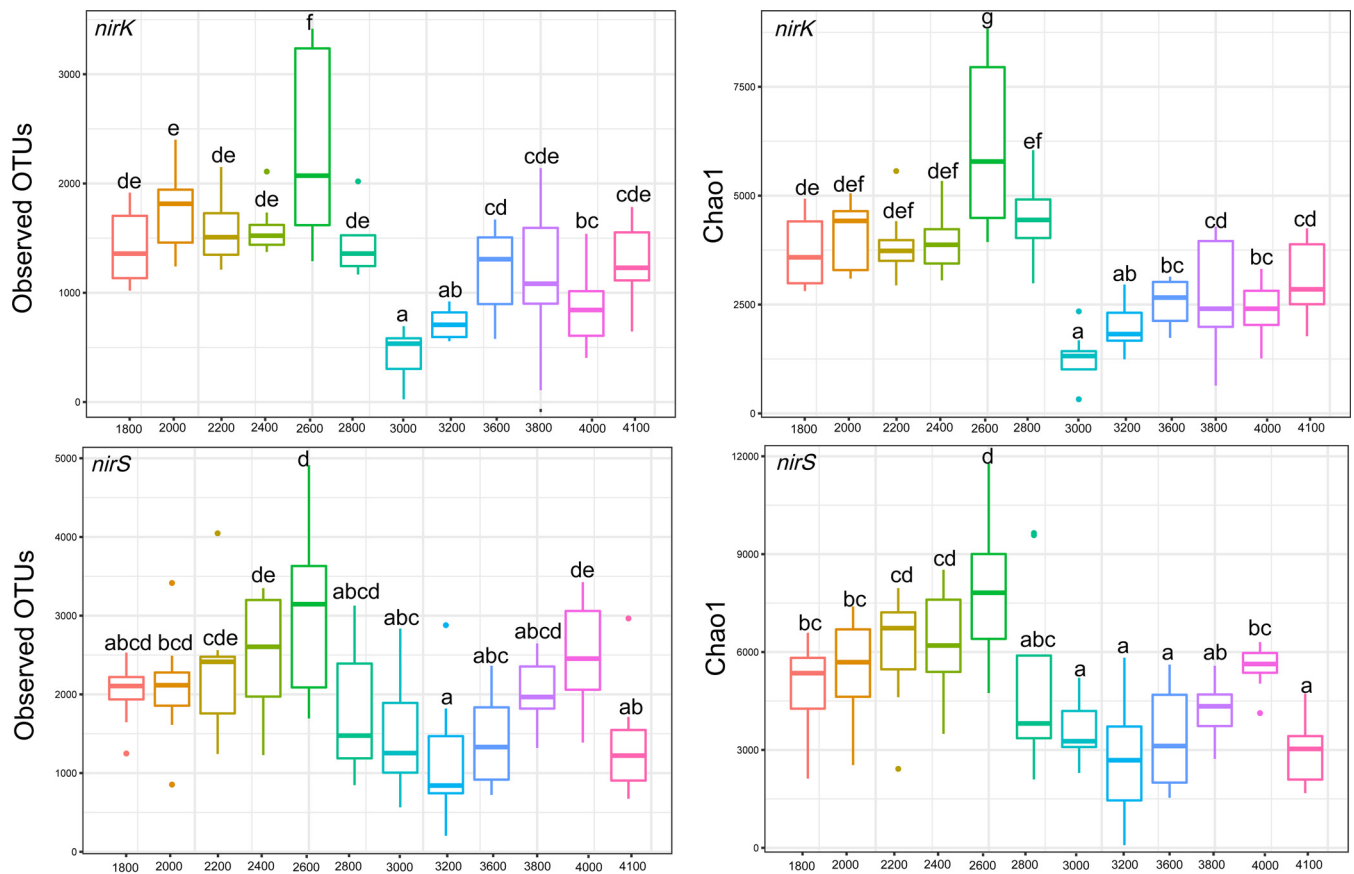


**FIG 1**  $\alpha$ -Diversity indices for *nirK*-type and *nirS*-type denitrifier communities, including observed operational taxonomic units (OTUs) and Chao1 along the elevation gradient.

**The  $\alpha$ -diversity, community composition, and abundances of *nirK*-type and *nirS*-type denitrifiers.** The  $\alpha$ -diversities of *nirK*-type and *nirS*-type denitrifier communities exhibited hump-backed patterns along the elevation gradient, and the peak values occurred at 2,600 and 3,800 m, respectively (Fig. 1). Moreover, an abrupt decrease in alpha diversity of denitrifier communities occurred between 2,600 and 2,800 m. However, the results of nonparametric multivariate analysis of variance (NPMANOVA) showed that the *nirK*-type and *nirS*-type denitrifier communities changed significantly with elevation, except for those in several neighboring sites (Fig. 2; see also Tables S1 and S2 in the supplemental material). The *nirK*-type denitrifier communities formed two distinct clusters that were primarily separated by elevation, and they were also separated by the presence of mixed forests of deciduous broadleaf and dark coniferous species at 2,800 m (Fig. 2). However, *nirS*-type denitrifier communities formed three distinct clusters that were separated primarily by deciduous broadleaf/dark coniferous forests and alpine shrub meadows along the elevation gradient (Fig. 2).

The *nirK*-type denitrifier communities were dominated by class *Alphaproteobacteria* (relative abundance, 63 to 88%) (Fig. S1), followed by *Betaproteobacteria* (3 to 10%) and *Gammaproteobacteria* (0.1 to 5%) (Fig. S1). In this study, the genera with relative abundance of  $\geq 0.05\%$  at least at one elevation were defined as major genera. The major genera of *nirK*-type denitrifiers were *Achromobacter*, *Bradyrhizobium*, *Chelativorans*, *Mesorhizobium*, *Nitrosomonas*, *Pseudomonas*, and *Rhodopseudomonas* (Fig. 3). The *nirS*-type denitrifier communities were dominated by classes *Betaproteobacteria* (23 to 82%) and *Gammaproteobacteria* (9 to 68%) (Fig. S1), whereas *Alphaproteobacteria* only accounted for 2 to 13% (Fig. S1). The major genera of *nirS*-type denitrifiers included *Azoarcus*, *Bordetella*, *Bradyrhizobium*, *Cupriavidus*, *Dechlorospirillum*, *Halomonas*, *Pseudomonas*, *Ralstonia*, *Rhodanobacter*, *Rubrivivax*, *Sulfuricaulis*, *Sulfuritalea*, and *Thaueria* (Fig. 3).

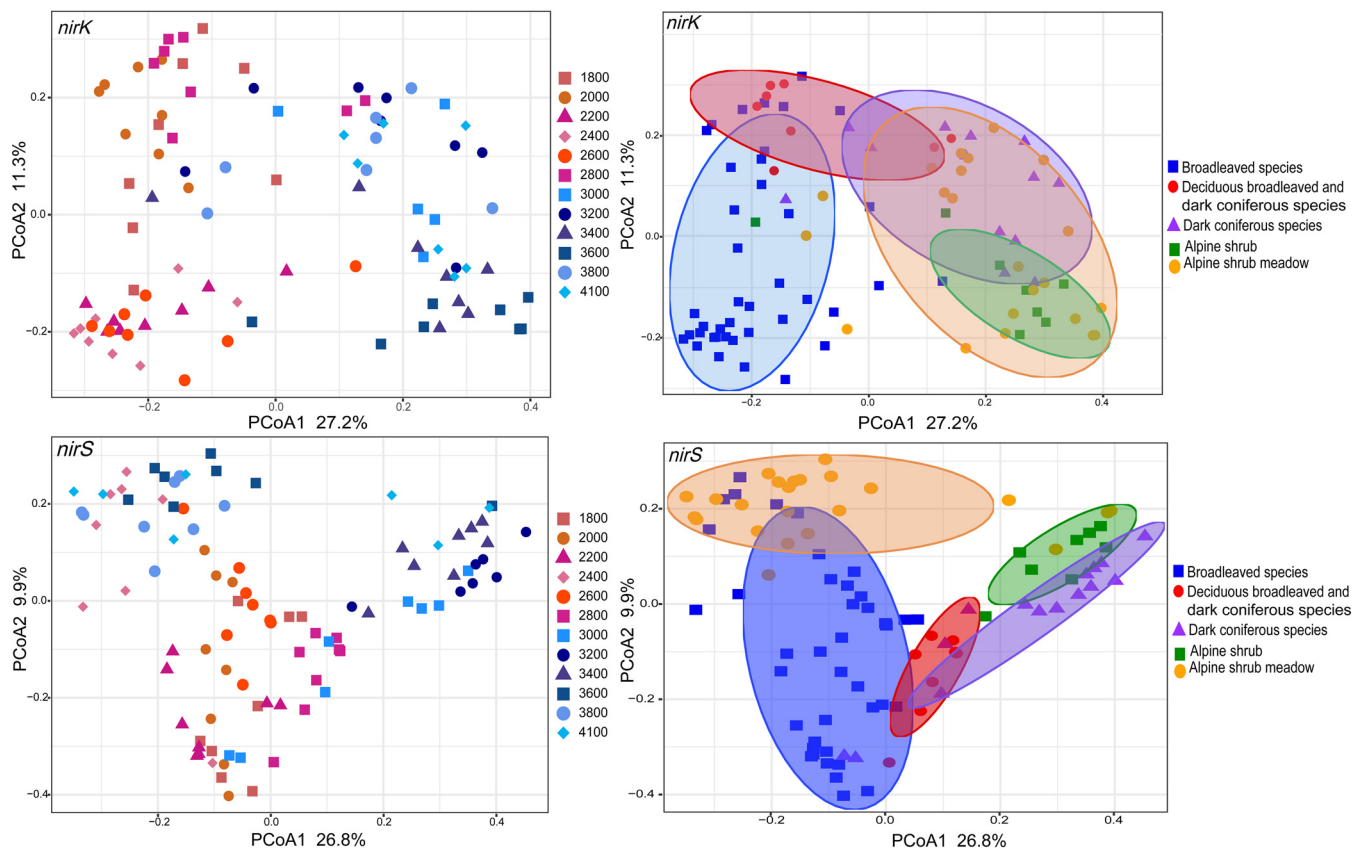


**FIG 2** Principal coordinate analysis (PCoA) of *nirK*-type and *nirS*-type denitrifier community composition along the elevation gradient, ranked by elevation (upper and lower right) and vegetation type (upper and lower left) based on the Bray-Curtis dissimilarity matrix. Ellipses were defined as 95% confidence intervals for the centroids of denitrifiers.

The different patterns of *nirK*-type and *nirS*-type denitrifiers along the elevation gradient were also reflected in specific taxa (Fig. S2 and S3). Among the major genera, only *Bradyrhizobium* and *Pseudomonas* occurred in both *nirK*-type and *nirS*-type denitrifier communities (Fig. 3). However, *nirK*-type denitrifiers in *Bradyrhizobium* and *Pseudomonas* showed response patterns to elevation differing from those of *nirS*-type denitrifiers. Specifically, the relative abundance of *nirK*-type *Bradyrhizobium* increased significantly with elevation, whereas the relative abundance of *nirS*-type *Bradyrhizobium* decreased significantly with elevation. The presence of *nirK*-type *Pseudomonas* was only detected at high elevations of 3,600 and 3,800 m, with relative abundance first increasing and then decreasing, whereas the relative abundance of *nirS*-type *Pseudomonas* increased at a low elevation and then decreased at elevations above 3,200 m (Fig. S2 and S3).

The numbers of copies of *nirK* and *nirS* genes decreased with increasing altitude, ranging from  $(1.40 \pm 0.46) \times 10^8$  to  $(8.89 \pm 4.89) \times 10^8$  copies  $g^{-1}$  dry soil and  $(1.05 \pm 0.26) \times 10^7$  to  $(1.05 \pm 6.61) \times 10^7$  copies  $g^{-1}$  dry soil, respectively (Table S3). The abundances of the *nirK* genes were  $16.67 \pm 9.82$  to  $44.99 \pm 11.77$  times greater than those of *nirS* genes at all elevations (Table S3).

**Ecological processes shaping denitrifier community assemblages.** For *nirK*-type and *nirS*-type denitrifier communities, the mean nearest taxon index (NTI) was 1.27 or 1.38, respectively ( $P < 0.05$ ), indicating that both *nirK*-type and *nirS*-type communities were phylogenetically clustered and that the assemblages of *nirK*-type and *nirS*-type denitrifier communities were affected mainly by environmental filtration. Moreover, based on the results of phylogenetic null model analysis, heterogeneous selection and homogeneous selection explained 40.9% and 18.2%, respectively, of the turnover in community composition for *nirK*-type denitrifiers, with 25.3%, 8.6%, and 7% explained by dispersal limitation, homogenizing dispersal, and undominated, respectively (Fig. 4).



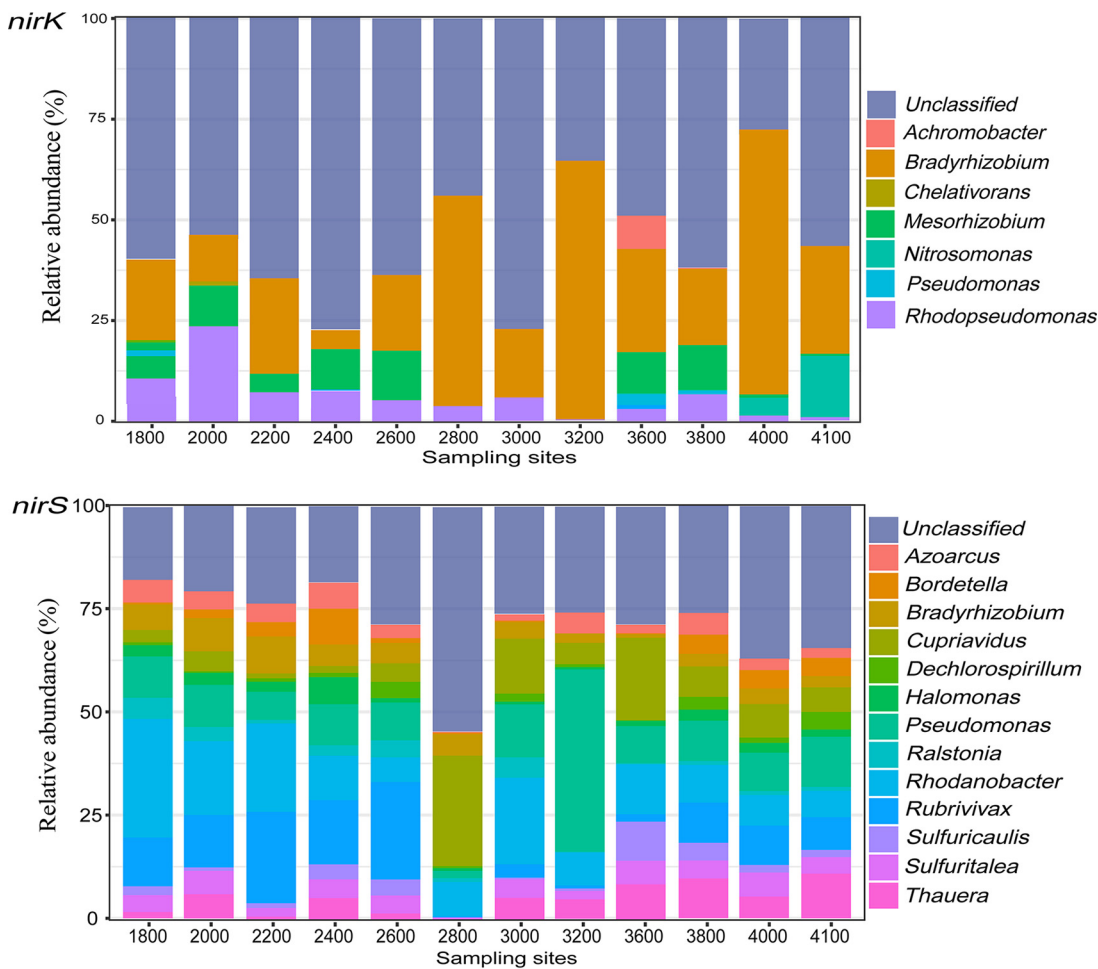


**FIG 3** Community composition of *nirK*-type and *nirS*-type denitrifiers at the genus level along an elevation gradient.

For the *nirS*-type denitrifier communities, heterogeneous and homogeneous selection explained 44.5% and 16.7% of the community turnover, followed by 21.4%, 9.8%, and 7.5% explained by dispersal limitation, homogenizing dispersal, and undominated, respectively (Fig. 4).

**Factors influencing the community composition and abundances of *nirK*-type and *nirS*-type denitrifiers along the elevation gradient.** Most observed environmental factors were significantly associated with community-level attributes and the abundances of denitrifiers (Table S4). Among all the variables, soil pH and the total diameter at breast height (DBH) in DC (DBH-DC) forest explained the most variation in the  $\alpha$ -diversity of *nirK*-type denitrifier communities, whereas plant richness was the main predictor of the  $\alpha$ -diversity of *nirS*-type denitrifiers (Table 1). In addition, the DBH in DB (DBH-DB) and TC/TN explained the most variation in number of copies of *nirK* (Table 1), whereas TN and plant richness were the major predictors for the *nirS* (Table 1). Soil pH showed a significant correlation with the relative abundances of *Bradyrhizobium*, *Chelativorans*, and *Rhodopseudomonas* in the *nirK*-type communities (Table S5), whereas plant richness was significantly correlated with the relative abundances of *Bradyrhizobium*, *Rubrivivax*, *Cupriavidus*, *Ralstonia*, *Halomonas*, and *Thauera* in the *nirS*-type communities (Table S6).

Partial least-squares path modeling (PLS\_PM) explained 89% and 82% of the variation in *nirK*-type and *nirS*-type denitrifier communities, respectively (Fig. 5) (goodness of fit = 0.69 and 0.72, respectively). Geographical distance (PCNM1) significantly influenced *nirK*-type denitrifiers directly or indirectly through its effect on climate (MAT), MAT significantly influenced *nirK*-type denitrifiers indirectly through its effect on plants, and plants significantly influenced *nirK*-type denitrifier communities directly or indirectly through their effects on

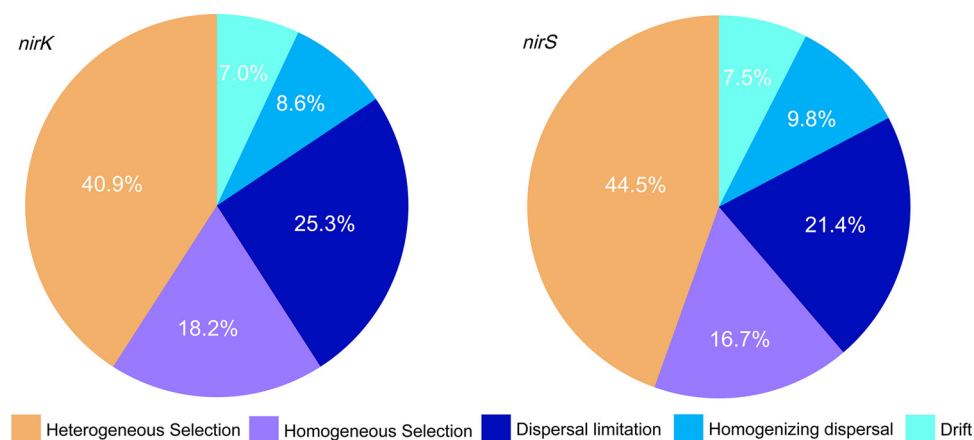


**FIG 4** Phylogenetic null model approach was used to quantify the relative contributions of deterministic processes (including heterogeneous selection and homogeneous selection) and stochastic processes (including dispersal limitation, homogenizing dispersal, and drift) to *nirK*-type and *nirS*-type denitrifier community assembly.

soil properties (Fig. 5). The direct effect of soil properties (path coefficient of 0.32) on the *nirK*-type denitrifiers exceeded those of PCNM1 (path coefficient of 0.26) and plants (path coefficient of 0.28) (Fig. 5). Among the environmental variables, soil pH was the most important factor shaping *nirK*-type communities (Fig. 6, Table 2).

Geographical distance (PCNM1) significantly influenced the *nirS*-type communities indirectly by its effect on climate (MAT). MAT significantly influenced *nirS*-type denitrifiers directly or indirectly by its effect on plants, and plants significantly influenced *nirS*-type denitrifier communities directly or indirectly by their effects on soil properties (Fig. 5). The direct effect of plants (path coefficient of  $-0.47$ ) on *nirS*-type denitrifiers was greater than those of MAT (path coefficient of  $-0.36$ ) and soil properties (path coefficient of  $-0.15$ ) (Fig. 5). Among the environmental variables, plant richness was the main factor shaping *nirS*-type denitrifier communities (Fig. 6, Table 2).

The results of cooccurrence network analysis showed that positive correlations dominated in relationships between *nirK*-type and *nirS*-type denitrifiers (Fig. S4). Moreover, plant richness played an important role in influencing the cooccurrence relationships between *nirK*-type and *nirS*-type denitrifiers (Fig. S4).

**TABLE 1** Roles of environmental variables on  $\alpha$ -diversity and copy numbers of the *nirK* and *nirS* genes evaluated by stepwise multivariate regression modeling

Gene	$\alpha$ -Diversity/copy no. test	Explanatory variable	Contribution of the individual predictor <sup>a</sup> (%)	P value	Adjusted R <sup>2</sup> for full model (P value)
<i>nirK</i>	Chao 1	pH	13.1	0.001	0.20 (<0.0001)
		DBH-DC	7.2	0.050	
	Observed OTUS	pH	10.6	0.012	
		DBH-DC	9.5	0.024	
	Copy no.	DBH-DB	19.2	0.028	
TC/TN		16.0	0.000		
<i>nirS</i>	Chao 1	Plant richness	30.1	0.000	0.40 (<0.0001)
		NO <sub>3</sub> <sup>-</sup> -N	9.9	0.002	
	Observed OTUS	Plant richness	15.9	0.000	
		NO <sub>3</sub> <sup>-</sup> -N	6.8	0.007	
		MAT	0.5	0.046	
	Copy no.	TN	21.3	0.001	
		Plant richness	17.4	0.008	
		Cond	7.5	0.008	
	DBH-EB	4.5	0.017		

<sup>a</sup>Percentage of the total sum of squares explained by each variable. DBH represents the total diameter at breast height, while DBH-DB, DBH-EB, and DBH-DC represent the percentage representation of deciduous broadleaf trees, evergreen broadleaf trees, and dark coniferous trees, respectively, in total DBH. TC, total carbon; TN, total nitrogen; MAT, mean annual temperature; Cond, Conductivity.

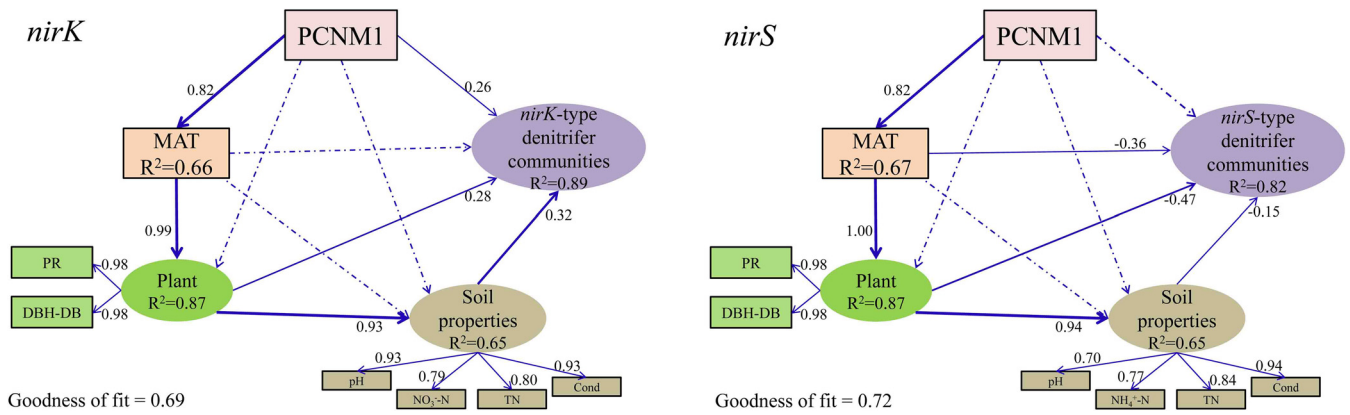


**FIG 5** Partial least-squares path modeling (PLS-PM) was used to estimate the direct and indirect effects of climatic, plant, and soil properties on *nirK*-type and *nirS*-type denitrifier communities. The width of an arrow represents the strength of the path coefficient. Continuous and dashed arrows indicate significant and nonsignificant path coefficients, respectively. PCNM1, principal component of neighbor matrices, representing geographical distance; MAT, mean annual temperature; PR, plant richness; TN, total nitrogen; Cond, conductivity. DBH represents the total diameter at breast height. DB represents the percentage of total DBH accounted for by deciduous broadleaf trees.

**Soil denitrification potential and its relationship with denitrifier communities and abundances.** Based on the acetylene inhibition technique, the PDR was estimated. The results showed that the PDR was significantly higher at low elevations (ranging from 21.30 to 285.96  $\mu\text{g N}_2\text{O-N g}^{-1}$  dry soil  $\text{h}^{-1}$ , 1,800 to 2,600 m) than at high elevations (ranging from 1.32 to 63.50  $\mu\text{g N}_2\text{O-N g}^{-1}$  dry soil  $\text{h}^{-1}$ , 2,800 to 4,100 m) (Fig. 7). Results of multiple regression on distance matrices (MRM) showed that the  $\beta$ -diversity of *nirK*-type and *nirS*-type denitrifier communities explained PDR well, and  $\beta$ -diversity of *nirK*-type denitrifier communities were more important in explaining PDR than were *nirS*-type denitrifiers (Fig. 6). However, the abundances and  $\alpha$ -diversity of *nirK*-type and *nirS*-type denitrifier communities did not show significant effects on PDR.

**DISCUSSION**

**The patterns of assembly of *nirK*-type and *nirS*-type denitrifier communities along the elevation gradient.** The  $\alpha$ -diversity of the *nirK*-type and *nirS*-type denitrifier communities showed hump-backed patterns along the elevation gradient. Moreover,

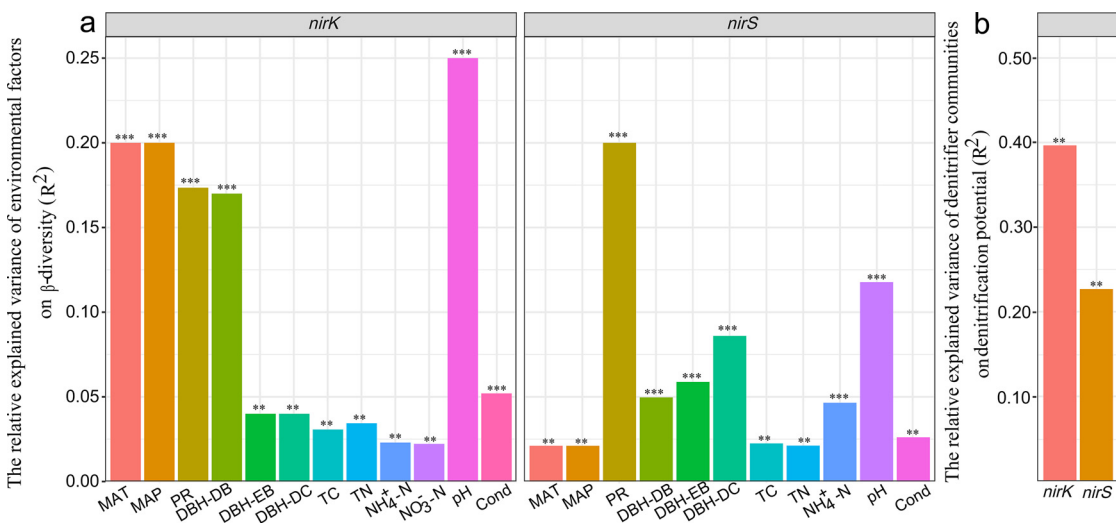


**FIG 6** Multiple regression on distance matrices (MRM) was used to estimate the relative proportions of variance explained by environmental factors in the turnover of *nirK*-type and *nirS*-type denitrifier communities along the altitudinal gradient and the relative variation in nitrification potential explained by *nirK*-type and *nirS*-type denitrifier communities (b) in the low- and high-altitudinal sections, respectively. MAT, mean annual temperature; MAP, mean annual precipitation; PR, plant richness; TC, total carbon; TN, total nitrogen; Cond, conductivity. DBH represents the total diameter at breast height. DB, EB, and DC represent the percent representations of deciduous broadleaf trees, evergreen broadleaf trees, and dark coniferous trees, respectively, in total DBH. \*\*,  $P < 0.01$ ; \*\*\*,  $P < 0.001$ .



**TABLE 2** Partial Mantel test analysis between the *nirK*- and *nirS*-type denitrifier communities and environmental factors along the elevation gradient<sup>a</sup>

Factor	<i>nirK</i> -type communities		<i>nirS</i> -type communities	
	pMantel.r	P value	pMantel.r	P value
Elevation	0.02	0.22	-0.07	1.00
Longitude	0.11	0.01*	0.24	0.00**
Latitude	0.07	0.04*	0.11	0.01*
pH	0.28	0.00**	0.29	0.00**
NH <sub>4</sub> <sup>+</sup> -N	0.10	0.02*	0.16	0.00**
NO <sub>3</sub> <sup>-</sup> -N	-0.04	0.76	0.10	0.04*
TC	0.03	0.23	0.12	0.01*
TN	0.03	0.20	0.11	0.01*
TC/TN	0.05	0.14	0.04	0.21
Conductivity	0.05	0.14	0.14	0.01*
MAT	-0.08	1.00	-0.10	1.00
MAP	0.02	0.21	-0.05	0.99
Plant richness	0.15	0.00**	0.36	0.00**
DBH-DB	0.03	0.23	0.19	0.00**
DBH-EB	0.03	0.26	0.18	0.00**
DBH-DC	0.13	0.00**	0.31	0.00**

<sup>a</sup>TC, total carbon; TN, total nitrogen; MAT, mean annual air temperature; MAP, mean annual precipitation. DBH represents the total diameter at breast height, while DBH-DB, DBH-EB, and DBH-DC represent the percent representation of deciduous broadleaf trees, evergreen broadleaf trees, and dark coniferous trees, respectively, in total DBH. \*, *P* < 0.05; \*\*, *P* < 0.01.

an abrupt decrease in the  $\alpha$ -diversity of denitrifier communities occurred between 2,600 and 2,800 m (Fig. 1). Similar patterns have also been reported for the elevational changes of soil bacteria (28), diazotrophs (25), and methanotrophs (24) along the same elevation gradient. Such a pattern of variation may be ascribed to the significant differences in soil properties (such as pH, NO<sub>3</sub><sup>-</sup>-N, TC, TN, and conductivity) between low (1,800 to 2,800 m) and high (3,000 to 4,100 m) elevations (23). Indeed, the variations in these soil properties significantly influenced *nirK*-type and *nirS*-type denitrifiers (Fig. 6; see also Tables S4 to S6 in the supplemental material), consistent with the findings of previous studies (7, 10–12). In addition, plants can influence *nirK*-type and *nirS*-type denitrifier communities (11, 14, 15). In this study, plants changed from mixed forests of

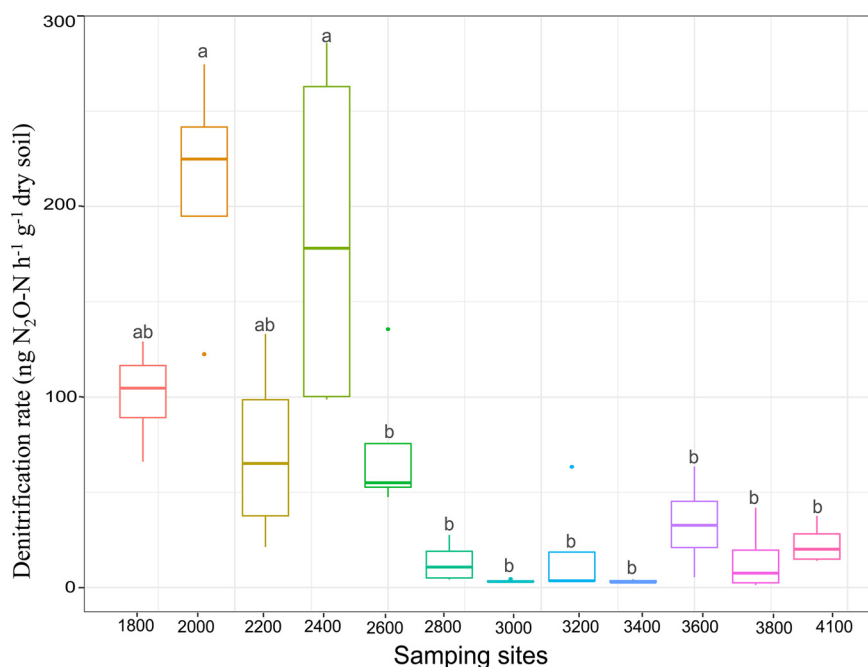


**FIG 7** Soil denitrification potential along the elevation gradient.

deciduous broadleaf and coniferous species to uniformly coniferous forests at 2,850 m, suggesting that the changes in plant community at approximately 2,850 m contribute to the differentiation in  $\alpha$ -diversity of denitrifier communities between low and high elevations. In addition to the contemporary factors described above, the elevational breakpoint of denitrifier diversity at approximately 2,800 m coincided with the Indus-Yalu suture zone fault in this region, which implies that past geological processes (e.g., parent rock and weathering) have left a strong signature on the elevational patterns of soil microbial diversity (27).

Moreover, *nirK*-type denitrifier communities formed two clusters at low (1,800 to 2,800 m) and high (3,000 to 4,100 m) elevational sections (Fig. 2). Similar results have been reported for the distribution of soil bacterial and methanotrophic communities along the same elevation gradients (23, 24), and differences in community structure between the lower and higher elevations were attributed mainly to changes in soil pH. However, unlike the *nirK*-type denitrifiers, three clusters of *nirS*-type denitrifier communities were observed along the elevation gradient (Fig. 2), which was consistent with the changes in plant communities. The differences in elevation pattern between the *nirS*-type and *nirK*-type denitrifier communities suggest that they are adapted to different ecological niches. *nirK*-type denitrifier communities were dominated by class *Alphaproteobacteria*, whereas the *nirS*-type denitrifier communities were dominated by classes *Betaproteobacteria* and *Gammaproteobacteria* (Fig. S1). This is consistent with the report by Heylen et al. (37). The major genera *Bradyrhizobium* and *Pseudomonas* showed different patterns of response to elevation between *nirK*-type and *nirS*-type denitrifiers (Fig. S2 and S3). The relative abundance of *nirK*-type *Bradyrhizobium* was primarily correlated with soil pH, whereas relative abundances of *nirS*-type *Bradyrhizobium* were primarily correlated with plant richness (Table S6). These results further support the possibility that they are adapted to different ecological niches.

**Deterministic processes dominating the assemblies of *nirK*-type and *nirS*-type denitrifier communities.** This study proved that *nirK*-type and *nirS*-type denitrifier communities were phylogenetically clustered. Deterministic processes (heterogeneous selection) were dominant in shaping *nirK*-type and *nirS*-type communities over the elevation gradient, and similar results have also been observed for soil bacteria (23, 30), diazotrophs (25), and methanotrophs (24) along the same elevation gradient. Furthermore, heterogeneous selection explained a high fraction of turnover in community composition of *nirK*-type and *nirS*-type denitrifiers (Fig. 4). These results provide partial support for hypothesis i. Natural selection was not able to explain denitrifier community structure completely because the drastic variation in climate, vegetation, and soil properties over a short spatial distance along the elevation gradient resulted in high variation in community structure. In addition, microbes may have ubiquitous dispersal capabilities due to their size and lower degree of restriction by geographical barriers (38); however, microbes have been recognized to be dispersal limited through a modeling approach (39). Indeed, this study demonstrated that dispersal limitation was also important in explaining the variations in the *nirK*-type and *nirS*-type denitrifier communities in montane ecosystems (Fig. 4). Therefore, our results confirmed the interactive effect of heterogeneous selection and dispersal limitation in shaping soil microbial communities.

**Different key drivers shifting *nirK*-type and *nirS*-type denitrifier communities.** Soil pH was the primary environmental variable explaining the variation in *nirK*-type denitrifier communities (Fig. 6, Tables 1 and 2). Indeed, previous studies have demonstrated the importance of pH in shaping denitrifier communities and other microbial groups in various ecosystems (4, 40, 41). Appropriate pH is crucial for the growth and activity of denitrifiers (4), and it is considered the primary variable that links soil organic matter recycling, plant nutrition, and plant-microbial interactions in soils (13, 42). For example, soil pH can influence the level of dissolved organic matter by affecting the sorption of dissolved organic matter components to soil molecules (13). Changes in nutrient availability can influence the abundances and community composition of denitrifiers (4). However, there is a debate about the relative effects of pH and climate (temperature) on soil microbial communities (43). In this study, PLS\_PM analysis

showed that the direct effect of a soil property (pH) on *nirK*-type denitrifier communities was greater than that of climate (Fig. 5). Moreover, soil pH showed a significant correlation with the relative abundances of *Bradyrhizobium*, *Chelativorans*, and *Rhodopseudomonas* (Table S5). These *nirK*-type denitrifiers were abundant generalists found in all the samples (Fig. S2). Therefore, soil pH may directly mediate *nirK*-type denitrifiers by species sorting mechanisms that shift the relative abundances of *Bradyrhizobium*, *Chelativorans*, and *Rhodopseudomonas*.

Plant richness was the main factor explaining the variation in the *nirS*-type denitrifier communities (Fig. 6, Tables 1 and 2). The results described above provide support for hypothesis i. The pattern of distribution of *nirS*-type denitrifiers was consistent with spatial variation in the plant community, which suggests that *nirS*-type denitrifiers are more sensitive to plant properties than are *nirK*-type denitrifiers in mountain ecosystems. Previous studies have reported *nirS*-type denitrifiers to be more closely associated than *nirK*-type denitrifiers with plants in forest soils (13), watershed soils (14), agricultural soils (11), and wetland soils (15), although some other studies have shown that *nirS*-type denitrifiers are sensitive to chemical and physical properties (44, 45). Genomic data have shown that the *nirS*-type denitrifiers may have a more complete denitrification pathway than that of *nirK*-type denitrifiers (46), and the majority of *nirS*-type denitrifiers are anaerobic heterotrophic microorganisms that can grow on the exudation of labile carbon (10, 11). Plants influence denitrifier communities not only by directly increasing the amount and quality of plant aboveground (litter) and belowground (root exudation) materials (11, 16, 47) but also by indirectly modifying soil physicochemical properties, including soil permeability, pH, substrate availability, and soil moisture (48–50). Plant richness was significantly correlated with the relative abundances of *Bradyrhizobium*, *Rubrivivax*, *Cupriavidus*, *Ralstonia*, *Halomonas*, and *Thauera* (Table S6), which were abundant *nirS*-type denitrifiers widely distributed along the elevation gradient (Fig. S3). Therefore, plants may directly influence *nirS*-type denitrifiers by shifting the abundances of these microbes and indirectly by their effects on soil properties. Additionally, plant richness also played an important role in influencing the cooccurrence of *nirK*-type and *nirS*-type denitrifiers along elevation gradients (Fig. S4), suggesting that the cooccurrence relationships between *nirK*-type and *nirS*-type denitrifiers will readily suffer the effects of variation in plant communities in mountain ecosystems in the future.

#### **Relationships between denitrifier communities and soil denitrification potential.**

In this study, the distinct changes in PDR were significantly associated with the changes in  $\beta$ -diversity of *nirK*-type and *nirS*-type denitrifier communities (Fig. 6). This provides partial support for hypothesis ii. This result was consistent with those of recent studies that have found *nirK*-type and *nirS*-type communities to play important roles in determining denitrification rates in grassland systems (35) and in pasture soils (32). Our results suggest that the predictive strength of models explaining facultative processes could be improved by taking into account denitrifier communities. Moreover, the  $\beta$ -diversity of the *nirK*-type denitrifiers explained more of the variation in PDR than did that of *nirS*-type denitrifiers, implicating more important roles of *nirK*-type denitrifiers in soil denitrification. This result did not support hypothesis ii, that the composition of *nirS*-type communities plays more important roles in explaining PDR. This result was also inconsistent with finding of previous studies that have reported that *nirS*-type denitrifiers were able to produce greater quantities of denitrification enzyme and, thus, maintain higher PDR (4) and that *nirS*-type denitrifiers are more likely than *nirK*-type denitrifiers to be capable of complete denitrification (36). These inconsistent results may be ascribed to the increased sensitivity to pH of transcription found in *nirS*-type denitrifiers, with transcription limited at low pH (for example, pH 4.7) (4, 51); therefore, *nirS*-type denitrifiers have poor capacity to reduce  $\text{NO}_2^-$  to NO at low pH values. Unlike *nirS*-type denitrifiers, *nirK*-type denitrifiers did not show sensitivity to soil pH; therefore, *nirK*-type denitrifiers may have a competitive advantage at low pH values. However, the abundances of denitrifiers did not show significant correlations with PDR. This finding is inconsistent with previous reports that gene abundance can be

used as an integrative ecological variable to predict the dynamics of PDR (1, 7, 33). This contradiction might be ascribed to the dominant effects of environmental variables on PDR, since the fluctuations of certain environmental factors (such as soil pH and total organic carbon) may result in simultaneous changes in the denitrification rate but not denitrifier gene abundances (33).

**Conclusions.** This study revealed elevation patterns of *nirK*-type and *nirS*-type denitrifier communities along the elevation gradient on Mount Gongga. We have found, for the first time, that deterministic processes, mainly heterogeneous selection, were more important than other processes in shaping the assemblies of *nirK*-type and *nirS*-type denitrifier communities. Moreover, the primary influencing variables were pH for *nirK*-type denitrifiers and plant richness for *nirS*-type denitrifiers. In addition, the  $\beta$ -diversity of *nirK*-type denitrifier communities explained more variation in PDR than that of *nirS*-type denitrifier communities. These results indicate close linkages among denitrifier diversity, climate, plant richness, and soil properties, which are critical for predicting the consequences of global changes on denitrifier communities and their ecological functions.

## MATERIALS AND METHODS

**Site description, sample collection, and soil characterization.** Mount Gongga (29°33' to 29°36' N, 101°57' to 102°05' E) is located on the eastern boundary of the Tibetan Plateau, Sichuan Province, southwest China. Mount Gongga is also the easternmost 7,556-m peak in the world and the third highest peak outside the Himalayan/Karakoram Range, after Tirich Mir and Kongur Tagh. The eastern slope of Mount Gongga is relatively steep (average slope, 75%), and the western slope is less steep (average slope, 25%). The mean annual temperature on the eastern slope of Mount Gongga decreases by 0.67°C when the elevation increases by 100 m, whereas the mean annual precipitation increases by 67.5 mm. Climatic and topographic variation create a vertical zonation of different forest types, with the vegetation on the east aspect of Mount Gongga representing the complete vegetation spectrum of the subtropical region in China. Evergreen broadleaf forests range from 1,200 to 1,800 m and mainly include *Lindera* spp., *Cinnamomum* spp., *Cyclobalanopsis* spp., etc. Mixed evergreen and deciduous broadleaf forests range from 1,800 to 2,500 m and mainly include *Lithocarpus cleistocarpus* and *Quercus* spp. Mixed forests of deciduous broadleaf and coniferous species range from 2,500 to 2,850 m and mainly include *Tsuga dumosa*, *Picea brachytyla*, and *Acer flabellatum*. From 2,850 m up to the treeline at approximately 3,850 m, the species *Abies fabri* is dominant in the subalpine forests. From 3,600 to 3,700 m, alpine shrubs (*Rhododendron lapponicum*) dominate in the lower region, and mixed mosaics of alpine shrubs and meadows range from 3,650 to 4,200 m (52).

Soil samples were collected in October 2014 from 12 sites along a 1,800- to 4,100-m elevation gradient with a pairwise interval of approximately 200 m along the east slope of Mount Gongga, as described by Li et al. (23). Briefly, at each sampling site, eight 10-m by 10-m plots were established. At each plot, five random soil core samples (0 to 10 cm) were collected using a soil corer (2.5-cm diameter) and then pooled as one composite sample for further analysis. Overall, 96 topsoil samples were collected from 12 sites along the elevation gradient. After passing through a 2-mm sieve, each fresh soil sample was separated into two parts, one of which was stored at 4°C for measuring soil physiochemical properties, whereas the other was stored at -40°C for molecular analysis.

The following climatic, plant, and soil properties were collected or determined and used in subsequent statistical analyses: latitude; longitude; elevation; MAT; MAP; TC, TN,  $\text{NH}_4^+$ , and  $\text{NO}_3^-$  concentrations; pH; and conductivity. Moreover, the plant species composition and richness were recorded in each plot (23). The diameter at breast height was measured for each woody plant, and the percentages of total DBH of EB, DB, and DC were calculated at each elevation based on the sum of diameters of all the woody plants at each elevation (23). Descriptions of climate data collection and plant and soil property measurements are available in Li et al. (23).

**DNA extraction and qPCR amplification.** Total soil DNA was extracted from 0.25 g soil using a MoBio Powersoil DNA isolation kit (San Diego, CA, USA) by following the manufacturer's instructions. The concentration and purity of the extracted DNA were quantified using a NanoDrop spectrophotometer and 1% agarose gels, and high-quality DNA was stored at -20°C for downstream analysis. The *nirK* and *nirS* genes were amplified using the primer pairs F1aCu/R3Cu (53) and cd3aF/R3cd (54), respectively. Quantitative PCR (qPCR) is an effective method and is widely used to determine the abundances of denitrifier genes (*nirK* and *nirS*) (1, 55). Despite its high variability, qPCR still allows for a comparative analysis of the relative abundance of each gene across the different soil samples (56). The reaction volume was 10  $\mu\text{l}$  and contained 0.5  $\mu\text{l}$  of each primer, 5  $\mu\text{l}$  of 2 $\times$  SYBR green qPCR master mix (Bio-Rad, USA), 2  $\mu\text{l}$  of DNA template, and 2  $\mu\text{l}$  of sterilized water. PCR was performed in a thermocycler for 5 min at 95°C, followed by 40 cycles of denaturation at 95°C for 30 s, annealing for 30 s (57 and 55°C for the *nirK* and *nirS* genes, respectively), and extension at 72°C for 30 s. Melting curve analysis was conducted after amplification. The qPCR standards for quantification were obtained from PCR amplification products of genes from environmental DNA using each primer set, and the detailed method is available in Kou et al.

(57). Amplification efficiencies were 99% and 98% for the *nirK* and *nirS* genes, respectively, with  $R^2$  values higher than 0.99 and no detection of signals in the negative controls.

**PCR amplification and MiSeq sequencing.** Amplification of *nirK* and *nirS* genes was performed using the gene primers F1aCu/R3Cu (53) and cd3aF/R3cd (54), respectively. The 25- $\mu$ l reaction system contained 0.3  $\mu$ M forward and reverse primers, 12.5  $\mu$ l of 2 $\times$  EasyTaq PCR SuperMix (TransGen Biotech, China), 25 ng DNA template, and sterile water. Thermal cycling included an initial denaturation at 95°C for 5 min, followed by 35 cycles of amplification (94°C for 30 s, 57°C for *nirK* gene or 55°C for *nirS* gene for 1 min, and 72°C for 3 min) and a final extension at 72°C for 8 min. Four replicate PCR products from the same DNA sample were pooled and purified using a DNA gel extraction kit (Axygen, USA) by following the manufacturer's instructions, and the concentration and purity of DNA were determined using a NanoDrop spectrophotometer. PCR products were mixed in equal amounts and sequenced with an Illumina MiSeq PE300 sequencer by following the 2  $\times$  300 bp paired-end sequencing protocol at Chengdu Institute of Biology, CAS, China. The error rate of the sequencing platform was 1.5% for *nirK* and 2.1% for *nirS*.

**Processing of sequence data.** The QIIME pipeline was used to analyze raw sequences according to the barcodes, with trimming and quality filtering (58). Reads containing any ambiguous bases or any nucleotide mismatches within the barcodes or primer sequences were removed prior to analysis. Reads longer than 300 nucleotides and with high average quality score ( $Q \geq 30$ ) were used for further analysis. Chimeric sequences (averages of 2.9 and 4.7% for the *nirK* and *nirS* genes, respectively) were removed using Usearch 8 (59). Nonchimeric sequences with frameshifts (averages of 7.3% for *nirK* and 8.3% for *nirS*) were discarded (60). The analysis described above resulted in 217,082 (*nirK*) and 280,487 (*nirS*) high-quality sequences. All samples were resampled to an equal depth of 1,500 sequences per sample. Operational taxonomic unit (OTU) clustering was performed at a 3% dissimilarity cutoff value based on the nucleotide sequences using the UCHIME algorithm (v4.2.40) (61). Furthermore, the databases for both the nucleotide sequence alignment and species assignments were extracted from NCBI (<http://www.ncbi.nlm.nih.gov/>) and the Ribosomal Database Project function gene pipeline (<http://fungene.cme.msu.edu/>) (11, 62). To reduce sequence redundancy in diversity computation, identical *nirK* and *nirS* sequences were dereplicated using PRINSEQ (63). Classification of OTUs was performed using BLAST and the lowest common ancestor (LCA) algorithm in MEGAN (64). Related scripts about the bioinformatic analysis of *nirK* and *nirS* genes are available at <http://egcloud.cib.cn> and <http://lxzgroup.cib.cas.cn/kytj/yjff/>.

**Estimation of ecological processes shaping community assembly.** A phylogenetic null model approach was used to quantify the ecological processes shaping community assembly (21, 65, 66). We calculated the nearest taxon index (NTI) of each sample and  $\beta$ -nearest taxon index ( $\beta$ NTI) for paired samples using the R functions "comdistnt" and "ses.mntd" in the package "picante" (67, 68). The NTI can be used to examine the average taxonomic distance between each species and its closest relative in the tree (69). In general, NTI values significantly greater than zero indicate phylogenetic clustering; conversely, NTI values significantly less than zero indicate greater influence of stochastic processes (21). If  $\beta$ NTI  $> 2$  or  $\beta$ NTI  $< -2$ , deterministic processes are the most important factors in community assembly (21), whereas if  $|\beta$ NTI|  $< 2$ , stochastic processes are critical in shaping community composition. Specifically, if  $\beta$ NTI  $> 2$ , pairwise comparisons were evaluated as the contribution of heterogeneous selection, whereas if  $\beta$ NTI  $< -2$ , pairwise comparisons were estimated as the contribution of homogeneous selection (21). The Raup-Crick metric incorporating the relative abundances of species ( $RC_{\text{bray}}$ ) was used to further quantify the stochastic processes (21). If  $|\beta$ NTI|  $< 2$  and  $RC_{\text{bray}} > 0.95$ , pairwise comparisons were quantified as the fraction of the dispersal limitation, whereas if  $|\beta$ NTI|  $< 2$  and  $RC_{\text{bray}} < -0.95$ , pairwise comparisons were quantified as homogenizing dispersal (21, 70). Finally, the fraction of the pairwise comparisons with  $|\beta$ NTI|  $< 2$  and  $|RC_{\text{bray}}| < 0.95$  was treated as undominated (70). The detailed script for the calculation process of ecological processes shaping community assembly can be found on GitHub (<https://github.com/Chiliubio/microeco>).

**Potential denitrification rate.** The PDR was determined using the acetylene inhibition technique (71). One hundred grams of fresh soil from each sample was weighed into a 1-liter glass bottle, and the soil moisture was adjusted to 60% of field capacity. Bottles were preincubated with loosely capped stoppers at 25°C for 1 week, and then soil equivalent to 20 g dry soil from each sample was transferred to a separate 250-ml serum bottle. A 5-ml solution containing 1,200  $\mu$ g ml<sup>-1</sup> glucose-C and 200  $\mu$ g ml<sup>-1</sup> NO<sub>3</sub><sup>-</sup>-N was added to each bottle (9, 72). All of the serum bottles were sealed and made anoxic by filling with pure N<sub>2</sub> gas (99.999%) for 2 min. Approximately 10% of the headspace of each bottle was replaced with acetylene to block the conversion of N<sub>2</sub>O to N<sub>2</sub> during denitrification. At the same time, the gas tightness of the incubation system was determined using a control bottle without soil. At 2 and 4 h, 10 ml headspace gas was taken from each bottle using a syringe. The N<sub>2</sub>O concentrations were measured using a gas chromatograph (GC; Shimadzu, Kyoto, Japan) equipped with an electron capture detector. The PDR values were calculated according to the change in the N<sub>2</sub>O concentration between the 2- and 4-h measurements (71).

**Statistical analyses.** The data were transformed by Box-Cox transformation and subjected to analysis of variance (ANOVA), and Tukey's *post hoc* test was performed to determine significant ( $P < 0.05$ ) effects. One-way analysis of variance was performed to estimate significant differences ( $P < 0.05$ ) in numbers of copies of *nirK* and *nirS* genes as well as in PDR among 12 different elevation gradients. Spearman's rank correlation analysis was performed to correlate environmental factors with  $\alpha$ -diversity indices, the relative abundances of the denitrifier taxa, denitrifier gene abundances, and PDR. The  $P$  values from the correlation analysis were adjusted according to the Benjamini-Hochberg false discovery rate (FDR) (73). Furthermore, stepwise multivariate regression modeling was used to identify the main



factors influencing the  $\alpha$ -diversity and numbers of copies of the *nirK* and *nirS* genes. Nonlinear fitting was performed between the relative abundances of major genera of *nirK*-type and *nirS*-type denitrifiers and elevation. The detailed scripts for the calculation process of nonlinear fitting are available at <http://lxzgroup.cib.cas.cn/kytj/yjff/>. Principal coordinate analysis (PCoA) based on Bray-Curtis distances was applied to explore the variation in denitrifier communities ( $\beta$ -diversity) along the elevation gradient. The statistical significance of differences among 12 elevations was assessed by NPMANOVA, with Bonferroni correction of *P* values for multiple comparisons, in PAST version 2.17.

We performed PLS\_PM (74) to evaluate the fit of the *nirK*-type/*nirS*-type denitrifier communities to geographical distance and measured environmental parameters. Principal components of neighbor matrices (PCNM) represent the geographical distance and were calculated using the function “pcnm” in the R package “vegan” (75). The models were constructed using the function “inner plot” in the R package “plsrm” (74). The method was described in detail by Kou et al. (57). In addition, MRM was performed to identify the main factors shaping the denitrifier communities at the OTU level using the “MRM” function in the R-library “ecodist.” Furthermore, the effects of variation in *nirK*-type/*nirS*-type denitrifier communities and numbers of copies of *nirK*-type/*nirS*-type denitrifiers on PDR were estimated by MRM. In the MRM model, Euclidean distance matrices and Bray-Curtis distance matrices were used for environmental factors and denitrifier communities, respectively. Partial Mantel test analysis between the *nirK*-type and *nirS*-type denitrifier communities and environmental factors was also performed to further identify the main factors shaping the denitrifier communities along the elevation gradient. In addition, the patterns of co-occurrence between *nirK*-type and *nirS*-type denitrifiers plus environmental factors were determined to further estimate the main factors shaping the denitrifier communities in the molecular ecological network analyses pipeline (MENAP) (<http://ieg2.ou.edu/MENA/main.cgi>) with random matrix theory (RMT)-based algorithms at the OTU level (76). Cytoscape 3.7.0 software was used to visualize the network graphs.

**Data availability.** The raw sequence data were stored in the European Nucleotide Archive under the accession number PRJEB30869 (<http://www.ebi.ac.uk/ena/data/view/PRJEB30869>).

## SUPPLEMENTAL MATERIAL

Supplemental material is available online only.

**FIG S1**, TIF file, 0.7 MB.

**FIG S2**, TIF file, 1 MB.

**FIG S3**, TIF file, 2.3 MB.

**FIG S4**, TIF file, 2.8 MB.

**TABLE S1**, DOCX file, 0.03 MB.

**TABLE S2**, DOCX file, 0.03 MB.

**TABLE S3**, DOCX file, 0.03 MB.

**TABLE S4**, DOCX file, 0.03 MB.

**TABLE S5**, DOCX file, 0.02 MB.

**TABLE S6**, DOCX file, 0.03 MB.

## ACKNOWLEDGMENTS

This work was supported by the National Natural Science Foundation of China (41601253, 31870473, and 31800519); the Youth Innovation Promotion Association, Chinese Academy of Sciences (2021371); the 13th 5-year Informatization Plan of Chinese Academy of Sciences (XXH13503-03-106); and China Biodiversity Observation Networks (Sino BON).

X.Z.L. and Y.P.K. planned and designed the research. Y.P.K., Y.J.L., J.B.L., C.N.L., B.T., and M.J.Y. performed experiments and collected data. Y.P.K. analyzed the data and wrote the manuscript. X.Z.L. and Y.P.K. revised the paper.

We declare that there are no conflicts of interest.

## REFERENCES

- Petersen DG, Blazewicz SJ, Firestone M, Herman DJ, Turetsky M, Waldrop M. 2012. Abundance of microbial genes associated with nitrogen cycling as indices of biogeochemical process rates across a vegetation gradient in Alaska. *Environ Microbiol* 14:993–1008. <https://doi.org/10.1111/j.1462-2920.2011.02679.x>.
- Philippot L. 2002. Denitrifying genes in bacterial and archaeal genomes. *Biochim Biophys Acta* 1577:355–376. [https://doi.org/10.1016/S0167-4781\(02\)00420-7](https://doi.org/10.1016/S0167-4781(02)00420-7).
- Kou YP, Wei K, Chen GX, Wang ZY, Xu H. 2015. Effects of 3,4-dimethylpyrazole phosphate and dicyandiamide on nitrous oxide emission in a greenhouse vegetable soil. *Plant Soil Environ* 61:29–35. <https://doi.org/10.17221/762/2014-PSE>.
- Herold MB, Giles ME, Alexander CJ, Baggs EM, Daniell TJ. 2018. Variable response of *nirK* and *nirS* containing denitrifier communities to long-term pH manipulation and cultivation. *FEMS Microbiol Lett* 365:fny035. <https://doi.org/10.1093/femsle/fny035>.
- Jones CM, Hallin S. 2010. Ecological and evolutionary factors underlying global and local assembly of denitrifier communities. *ISME J* 4:633. <https://doi.org/10.1038/ismej.2009.152>.
- Sánchez C, Minamisawa K. 2018. Redundant roles of Bradyrhizobium oligotrophicum Cu-type (*nirK*) and cd 1-type (*nirS*) nitrite reductase genes under denitrifying conditions. *FEMS Microbiol Lett* 365:fny015. <https://doi.org/10.1093/femsle/fny015>.

7. Xiong ZQ, Guo LD, Zhang QF, Liu GH, Liu WZ. 2017. Edaphic conditions regulate denitrification directly and indirectly by altering denitrifier abundance in wetlands along the Han River, China. *Environ Sci Technol* 51: 5483–5491. <https://doi.org/10.1021/acs.est.6b06521>.
8. Li BX, Chen JF, Wu Z, Wu SF, Xie SG, Liu Y. 2018. Seasonal and spatial dynamics of denitrification rate and denitrifier community in constructed wetland treating polluted river water. *Int Biodeter Biodegr* 126:143–151. <https://doi.org/10.1016/j.ibiod.2017.10.008>.
9. Kou YP, Li CN, Li JB, Tu B, Wang YS, Li XZ. 2019. Climate and soil parameters are more important than denitrifier abundances in controlling potential denitrification rates in Chinese grassland soils. *Sci Total Environ* 669: 62–69. <https://doi.org/10.1016/j.scitotenv.2019.03.093>.
10. Azziz G, Monza J, Etchebehere C, Irisarri P. 2017. *nirS*- and *nirK*-type denitrifier communities are differentially affected by soil type, rice cultivar and water management. *Eur J Soil Biol* 78:20–28. <https://doi.org/10.1016/j.ejsobi.2016.11.003>.
11. Hou SP, Ai C, Zhou W, Liang GQ, He P. 2018. Structure and assembly cues for rhizospheric *nirK*- and *nirS*-type denitrifier communities in long-term fertilized soils. *Soil Biol Biochem* 119:32–40. <https://doi.org/10.1016/j.soilbio.2018.01.007>.
12. Assémien FL, Cantarel AAM, Florio A, Lerondelle C, Pommier T, Gonnelly JT, Le Roux X. 2019. Different groups of nitrite-reducers and N<sub>2</sub>O-reducers have distinct ecological niches and functional roles in West African cultivated soils. *Soil Biol Biochem* 129:39–47. <https://doi.org/10.1016/j.soilbio.2018.11.003>.
13. Bárta J, Melichova T, Vanek D, Pícek T, Santruckova H. 2010. Effect of pH and dissolved organic matter on the abundance of *nirK* and *nirS* denitrifiers in spruce forest soil. *Biogeochemistry* 101:123–132. <https://doi.org/10.1007/s10533-010-9430-9>.
14. Guo GX, Deng H, Qiao M, Yao HY, Zhu YG. 2013. Effect of long-term wastewater irrigation on potential denitrification and denitrifying communities in soils at the watershed scale. *Environ Sci Technol* 47:3105–3113. <https://doi.org/10.1021/es304714a>.
15. Wu HL, Wang XZ, He XJ, Zhang SB, Liang RB, Shen J. 2017. Effects of root exudates on denitrifier gene abundance, community structure and activity in a micro-polluted constructed wetland. *Sci Total Environ* 598: 697–703. <https://doi.org/10.1016/j.scitotenv.2017.04.150>.
16. Kaiser C, Kilburn MR, Clode PL, Fuchslueger L, Koranda M, Cliff JB, Solaiman ZM, Murphy DV. 2015. Exploring the transfer of recent plant photosynthates to soil microbes: mycorrhizal pathway vs direct root exudation. *New Phytol* 205:1537–1551. <https://doi.org/10.1111/nph.13138>.
17. Bañeras L, Ruiz-Rueda O, Lopez-Flores R, Quintana XD, Hallin S. 2012. The Role of plant type and salinity in the selection for the denitrifying community structure in the rhizosphere of wetland vegetation. *Int Microbiol* 15:89–99.
18. Hu XJ, Liu JJ, Wei D, Zhu P, Cui XA, Zhou BK, Chen XL, Jin J, Liu XB, Wang GH. 2020. Chronic effects of different fertilization regimes on *nirS*-type denitrifier communities across the black soil region of Northeast China. *Pedosphere* 30:73–86. [https://doi.org/10.1016/S1002-0160\(19\)60840-4](https://doi.org/10.1016/S1002-0160(19)60840-4).
19. Jha N, Palmada T, Berben P, Saggari S, Luo JF, McMillan AMS. 2020. Influence of liming-induced pH changes on nitrous oxide emission, *nirS*, *nirK* and *nosZ* gene abundance from applied cattle urine in allophanic and fluvial grazed pasture soils. *Biol Fertil Soils* 56:811–824. <https://doi.org/10.1007/s00374-020-01460-1>.
20. Ligi T, Truu M, Truu J, Nolvak H, Kaasik A, Mitsch WJ, Mander U. 2014. Effects of soil chemical characteristics and water regime on denitrification genes (*nirS*, *nirK*, and *nosZ*) abundances in a created riverine wetland complex. *Ecol Eng* 72:47–55. <https://doi.org/10.1016/j.ecoleng.2013.07.015>.
21. Stegen JC, Lin XJ, Konopka AE, Fredrickson JK. 2012. Stochastic and deterministic assembly processes in subsurface microbial communities. *ISME J* 6:1653. <https://doi.org/10.1038/ismej.2012.22>.
22. Graham EB, Crump AR, Resch CT, Fansler S, Arntzen E, Kennedy DW, Fredrickson JK, Stegen JC. 2017. Deterministic influences exceed dispersal effects on hydrologically-connected microbiomes. *Environ Microbiol* 19: 1552–1567. <https://doi.org/10.1111/1462-2920.13720>.
23. Li JB, Shen ZH, Li CN, Kou YP, Wang YS, Tu B, Zhang SH, Li XZ. 2018. Stair-step pattern of soil bacterial diversity mainly driven by pH and vegetation types along the elevational gradients of Gongga Mountain. *Front Microbiol* 9:569. <https://doi.org/10.3389/fmicb.2018.00569>.
24. Li CN, Tu B, Kou YP, Wang YS, Li XZ, Wang JM, Li JB. 2021. The assembly of methanotrophic communities regulated by soil pH in a mountain ecosystem. *Catena* 196:104883. <https://doi.org/10.1016/j.catena.2020.104883>.
25. Wang YS, Li CN, Shen ZH, Rui JP, Jin DC, Li JB, Li XZ. 2019. Community assemblage of free-living diazotrophs along the elevational gradient of Mount Gongga. *Soil Ecol Lett* 1:136–146. <https://doi.org/10.1007/s42832-019-0013-y>.
26. Sundqvist MK, Sanders NJ, Wardle DA. 2013. Community and ecosystem responses to elevational gradients: processes, mechanisms, and insights for global change. *Annu Rev Ecol Evol Syst* 44:261–280. <https://doi.org/10.1146/annurev-ecolsys-110512-135750>.
27. Hu A, Wang JJ, Sun H, Niu B, Si GC, Wang J, Yeh CF, Zhu XX, Lu XC, Zhou JZ, Yang YP, Ren ML, Hu YL, Dong HL, Zhang GX. 2020. Mountain biodiversity and ecosystem functions: interplay between geology and contemporary environments. *ISME J* 14:931–944. <https://doi.org/10.1038/s41396-019-0574-x>.
28. Peay KG, von Sperber C, Cardarelli E, Toju H, Francis CA, Chadwick OA, Vitousek PM. 2017. Convergence and contrast in the community structure of Bacteria, Fungi and Archaea along a tropical elevation-climate gradient. *FEMS Microbiol Ecol* 93:fx045. <https://doi.org/10.1093/femsec/fix045>.
29. Shigyo N, Umeki K, Hirao T. 2019. Plant functional diversity and soil properties control elevational diversity gradients of soil bacteria. *FEMS Microbiol Ecol* 95:fiz025. <https://doi.org/10.1093/femsec/fiz025>.
30. Zhu BJ, Li CN, Wang JM, Li JB, Li XZ. 2020. Elevation rather than season determines the assembly and co-occurrence patterns of soil bacterial communities in forest ecosystems of Mount Gongga. *Appl Microbiol Biotechnol* 104:7589–7602. <https://doi.org/10.1007/s00253-020-10783-w>.
31. Mori AS, Isbell F, Seidl R. 2018.  $\beta$ -Diversity, community assembly, and ecosystem functioning. *Trends Ecol Evol* 33:549–564. <https://doi.org/10.1016/j.tree.2018.04.012>.
32. Samad MS, Bakken LR, Nadeem S, Clough TJ, de Klein CAM, Richards KG, Lanigan GJ, Morales SE. 2016. High-resolution denitrification kinetics in pasture soils link N<sub>2</sub>O emissions to pH, and denitrification to C mineralization. *PLoS One* 11:e0151713. <https://doi.org/10.1371/journal.pone.0151713>.
33. Wang HL, Shu DT, Liu D, Liu S, Den N, An SS. 2019. Passive and active ecological restoration strategies for abandoned farmland leads to shifts in potential soil nitrogen loss by denitrification and soil denitrifying microbes. *Land Degrad Dev* <https://doi.org/10.1002/ldr.3523>.
34. Tang YG, Yu GR, Zhang XY, Wang QF, Tian DS, Tian J, Niu SL, Ge JP. 2019. Environmental variables better explain changes in potential nitrification and denitrification activities than microbial properties in fertilized forest soils. *Sci Total Environ* 647:653–662. <https://doi.org/10.1016/j.scitotenv.2018.07.437>.
35. Cuhel J, Simek M, Laughlin RJ, Bru D, Cheneby D, Watson CJ, Philippot L. 2010. Insights into the effect of soil pH on N<sub>2</sub>O and N<sub>2</sub> emissions and denitrifier community size and activity. *Appl Environ Microbiol* 76:1870–1878. <https://doi.org/10.1128/AEM.02484-09>.
36. Graf DRH, Jones CM, Hallin S. 2014. Intergenomic comparisons highlight modularity of the denitrification pathway and underpin the importance of community structure for N<sub>2</sub>O emissions. *PLoS One* 9:e114118. <https://doi.org/10.1371/journal.pone.0114118>.
37. Heylen K, Gevers D, Vanparys B, Wittebolle L, Geets J, Boon N, De Vos P. 2006. The incidence of *nirS* and *nirK* and their genetic heterogeneity in cultivated denitrifiers. *Environ Microbiol* 8:2012–2021. <https://doi.org/10.1111/j.1462-2920.2006.01081.x>.
38. O'Malley MA. 2008. “Everything is everywhere: but the environment selects.” ubiquitous distribution and ecological determinism in microbial biogeography. *Stud Hist Philos Biomed Sci* 39:314–325. <https://doi.org/10.1016/j.shpsc.2008.06.005>.
39. Wilkinson DM, Koumoutsaris S, Mitchell EAD, Bey I. 2012. Modelling the effect of size on the aerial dispersal of microorganisms. *J Biogeogr* 39: 89–97. <https://doi.org/10.1111/j.1365-2699.2011.02569.x>.
40. Wang YS, Li CN, Kou YP, Wang JJ, Tu B, Li H, Li XZ, Wang CT, Yao MJ. 2017. Soil pH is a major driver of soil diazotrophic community assembly in Qinghai-Tibet alpine meadows. *Soil Biol Biochem* 115:547–555. <https://doi.org/10.1016/j.soilbio.2017.09.024>.
41. Cho HJ, Tripathi BM, Moroenyana I, Takahashi K, Kerfahi D, Dong K, Adams JM. 2019. Soil pH rather than elevation determines bacterial phylogenetic community assembly on Mt. Norikura. *FEMS Microbiol Ecol* 95: fty216. <https://doi.org/10.1093/femsec/fty216>.
42. Truong C, Gabbardini LA, Corrales A, Mujic AB, Escobar JM, Moretto A, Smith ME. 2019. Ectomycorrhizal fungi and soil enzymes exhibit contrasting patterns along elevation gradients in southern Patagonia. *New Phytol* 222:1936–1950. <https://doi.org/10.1111/nph.15714>.
43. Garcia-Pichel F, Loza V, Marusenko Y, Mateo P, Potrafka RM. 2013. Temperature drives the continental-scale distribution of key microbes in topsoil communities. *Science* 340:1574–1577. <https://doi.org/10.1126/science.1236404>.
44. Yin C, Fan FL, Song AL, Cui PY, Li TQ, Liang YC. 2015. Denitrification potential under different fertilization regimes is closely coupled with changes

- in the denitrifying community in a black soil. *Appl Microbiol Biotechnol* 99:5719–5729. <https://doi.org/10.1007/s00253-015-6461-0>.
45. Bowen H, Maul JE, Poffenbarger H, Mirsky S, Cavigelli M, Yarwood S. 2018. Spatial patterns of microbial denitrification genes change in response to poultry litter placement and cover crop species in an agricultural soil. *Biol Fertil Soils* 54:769–781. <https://doi.org/10.1007/s00374-018-1301-x>.
  46. Jones CM, Stres B, Rosenquist M, Hallin S. 2008. Phylogenetic analysis of nitrite, nitric oxide, and nitrous oxide respiratory enzymes reveal a complex evolutionary history for denitrification. *Mol Biol Evol* 25:1955–1966. <https://doi.org/10.1093/molbev/msn146>.
  47. Langarica-Fuentes A, Manrubia M, Giles ME, Mitchell S, Daniell TJ. 2018. Effect of model root exudate on denitrifier community dynamics and activity at different water-filled pore space levels in a fertilised soil. *Soil Biol Biochem* 120:70–79. <https://doi.org/10.1016/j.soilbio.2018.01.034>.
  48. Thoms C, Gattinger A, Jacob M, Thomas FM, Gleixner G. 2010. Direct and indirect effects of tree diversity drive soil microbial diversity in temperate deciduous forest. *Soil Biol Biochem* 42:1558–1565. <https://doi.org/10.1016/j.soilbio.2010.05.030>.
  49. Malique F, Butterbachbah K, Dannenmann M. 2017. Plant effects on soil denitrification—a review of potential mechanisms. *EGU Gen Assembly Conf Abstr*, p 6398.
  50. Moreau D, Bardgett RD, Finlay RD, Jones DL, Philippot L. 2019. A plant perspective on nitrogen cycling in the rhizosphere. *Funct Ecol* 33:540–552. <https://doi.org/10.1111/1365-2435.13303>.
  51. Brenzinger K, Dorsch P, Braker G. 2015. pH-driven shifts in overall and transcriptionally active denitrifiers control gaseous product stoichiometry in growth experiments with extracted bacteria from soil. *Front Microbiol* 6:961. <https://doi.org/10.3389/fmicb.2015.00961>.
  52. Shen ZH, Liu ZL, Wu J. 2004. Altitudinal pattern of flora on the eastern slope of Mt. Gongga. *Biodiversity Sci* 12:89–98. <https://doi.org/10.2116/analsci.20.717>.
  53. Hallin S, Lindgren PE. 1999. PCR detection of genes encoding nitrite reductase in denitrifying bacteria. *Appl Environ Microbiol* 65:1652–1657. <https://doi.org/10.1128/AEM.65.4.1652-1657.1999>.
  54. Throbäck IN, Enwall K, Jarvis A, Hallin S. 2004. Reassessing PCR primers targeting *nirS*, *nirK* and *nosZ* genes for community surveys of denitrifying bacteria with DGGE. *FEMS Microbiol Ecol* 49:401–417. <https://doi.org/10.1016/j.femsec.2004.04.011>.
  55. Jones CM, Spor A, Brennan FP, Breuil MC, Bru D, Lemanceau P, Griffiths B, Hallin S, Philippot L. 2014. Recently identified microbial guild mediates soil N<sub>2</sub>O sink capacity. *Nat Clim Chang* 4:801–805. <https://doi.org/10.1038/nclimate2301>.
  56. Penton CR, Johnson TA, Quensen JF, Iwai S, Cole JR, Tiedje JM. 2013. Functional genes to assess nitrogen cycling and aromatic hydrocarbon degradation: primers and processing matter. *Front Microbiol* 4:e00279. <https://doi.org/10.3389/fmicb.2013.00279>.
  57. Kou YP, Li JB, Wang YS, Li CA, Tu B, Yao MJ, Li XZ. 2017. Scale-dependent key drivers controlling methane oxidation potential in Chinese grassland soils. *Soil Biol Biochem* 111:104–114. <https://doi.org/10.1016/j.soilbio.2017.04.005>.
  58. Caporaso JG, Kuczynski J, Stombaugh J, Bittinger K, Bushman FD, Costello EK, Fierer N, Pena AG, Goodrich JK, Gordon JI, Huttley GA, Kelley ST, Knights D, Koenig JE, Ley RE, Lozupone CA, McDonald D, Muegge BD, Pirrung M, Reeder J, Sevinsky JR, Tumbaugh PJ, Walters WA, Widmann J, Yatsunenkov T, Zaneveld J, Knight R. 2010. QIIME allows analysis of high-throughput community sequencing data. *Nat Methods* 7:335–336. <https://doi.org/10.1038/nmeth.f.303>.
  59. Edgar RC. 2010. Search and clustering orders of magnitude faster than BLAST. *Bioinformatics* 26:2460–2461. <https://doi.org/10.1093/bioinformatics/btq461>.
  60. Wang Q, Quensen JF, Fish JA, Lee TK, Sun YN, Tiedje JM, Cole JR. 2013. Ecological patterns of *nifH* genes in four terrestrial climatic zones explored with targeted metagenomics using FrameBot, a new informatics tool. *mBio* 4:e00592-13. <https://doi.org/10.1128/mBio.00592-13>.
  61. Edgar RC, Haas BJ, Clemente JC, Quince C, Knight R. 2011. UCHIME improves sensitivity and speed of chimera detection. *Bioinformatics* 27:2194–2200. <https://doi.org/10.1093/bioinformatics/btr381>.
  62. Rui JP, Li JB, Wang SP, An JX, Liu WT, Lin QY, Yang YF, He ZL, Li XZ. 2015. Responses of bacterial communities to simulated climate changes in Alpine meadow soil of the Qinghai-Tibet Plateau. *Appl Environ Microbiol* 81:6070–6077. <https://doi.org/10.1128/AEM.00557-15>.
  63. Schmieder R, Edwards R. 2011. Quality control and preprocessing of metagenomic datasets. *Bioinformatics* 27:863–864. <https://doi.org/10.1093/bioinformatics/btr026>.
  64. Dumont MG, Luke C, Deng YC, Frenzel P. 2014. Classification of *pmoA* amplicon pyrosequences using BLAST and the lowest common ancestor method in MEGAN. *Front Microbiol* 5:34. <https://doi.org/10.3389/fmicb.2014.00034>.
  65. Kembel SW. 2009. Disentangling niche and neutral influences on community assembly: assessing the performance of community phylogenetic structure tests. *Ecol Lett* 12:949–960. <https://doi.org/10.1111/j.1461-0248.2009.01354.x>.
  66. Cadotte MW, Davies TJ, Regetz J, Kembel SW, Cleland E, Oakley TH. 2010. Phylogenetic diversity metrics for ecological communities: integrating species richness, abundance and evolutionary history. *Ecol Lett* 13:96–105. <https://doi.org/10.1111/j.1461-0248.2009.01405.x>.
  67. Fine PVA, Kembel SW. 2011. Phylogenetic community structure and phylogenetic turnover across space and edaphic gradients in western Amazonian tree communities. *Ecography* 34:552–565. <https://doi.org/10.1111/j.1600-0587.2010.06548.x>.
  68. Kembel SW, Kembel MSW. 2019. Package picante. <https://doi.org/10.1111/j.1461-0248.2009.01354.x>.
  69. Webb CO. 2000. Exploring the phylogenetic structure of ecological communities: an example for rain forest trees. *Am Nat* 156:145–155. <https://doi.org/10.1086/303378>.
  70. Zhou JZ, Ning DL. 2017. Stochastic community assembly: does it matter in microbial ecology? *Microbiol Mol Biol R* 81:e00002-17. <https://doi.org/10.1128/MMBR.00002-17>.
  71. Shrewsbury LH, Smith JL, Huggins DR, Carpenter-Boggs L, Reardon CL. 2016. Denitrifier abundance has a greater influence on denitrification rates at larger landscape scales but is a lesser driver than environmental variables. *Soil Biol Biochem* 103:221–231. <https://doi.org/10.1016/j.soilbio.2016.08.016>.
  72. Luo J, White RE, Ball PR, Tillman RW. 1996. Measuring denitrification activity in soils under pasture: optimizing conditions for the short-term denitrification enzyme assay and effects of soil storage on denitrification activity. *Soil Biol Biochem* 28:409–417. [https://doi.org/10.1016/0038-0717\(95\)00151-4](https://doi.org/10.1016/0038-0717(95)00151-4).
  73. Benjamini Y, Krieger AM, Yekutieli D. 2006. Adaptive linear step-up procedures that control the false discovery rate. *Biometrika* 93:491–507. <https://doi.org/10.1093/biomet/93.3.491>.
  74. Sanchez G. 2013. PLS path modeling with R. Trowchez Editions, Berkeley, CA.
  75. Borcard D, Legendre P. 2002. All-scale spatial analysis of ecological data by means of principal coordinates of neighbour matrices. *Ecol Model* 153:51–68. [https://doi.org/10.1016/S0304-3800\(01\)00501-4](https://doi.org/10.1016/S0304-3800(01)00501-4).
  76. Deng Y, Jiang YH, Yang YF, He ZL, Luo F, Zhou JZ. 2012. Molecular ecological network analyses. *BMC Bioinformatics* 13:113. <https://doi.org/10.1186/1471-2105-13-113>.